Supporting Information

Mechanism of methanol synthesis from CO_2 on Cu/CeO_2 and Cu/ W-CeO_2: A DFT investigation into the nature of W-doping

Nana Ma,[a] Weiyi Cheng,[a] Changgeng Wei,[b] Shujun Li,[a] and Guisheng Zhang*[a]*

[a]School of Chemistry and Chemical Engineering, Key Laboratory of Green Chemical Media and Reactions, Ministry of Education; NMPA Key Laboratory for Research and Evaluation of Innovative Drug, Henan Normal University, Xinxiang, Henan, 453007, China. E-mail: mann076@htu.edu.cn; zgs6668@yahoo.com.

[b]Bremen Center for Computational Materials Science, University of Bremen, 28359, Bremen, Germany.

Content

Cu_1/CeO_2-O_v

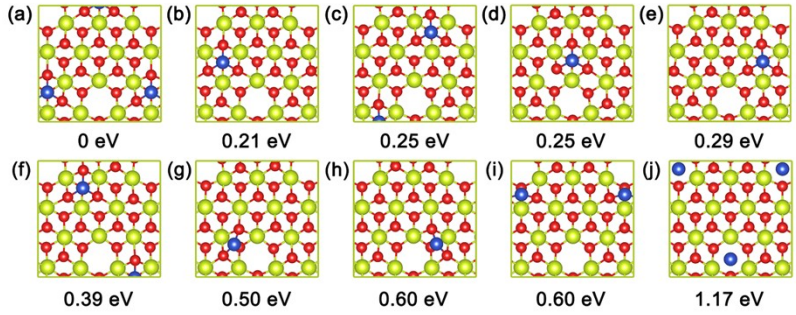

Cu_2/CeO_2-O_v

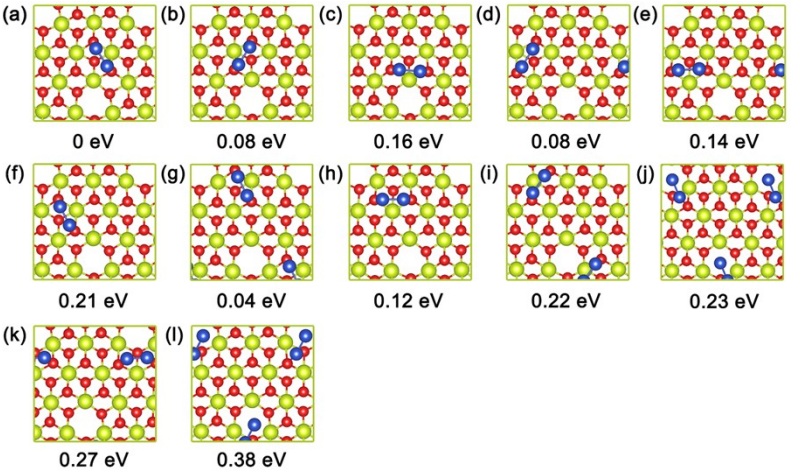

Cu_3/CeO_2-O_v

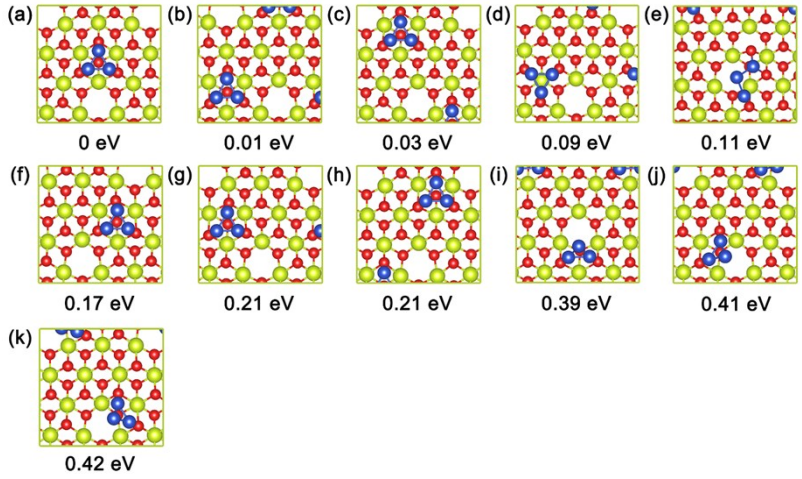

Cu_4/CeO_2-O_v

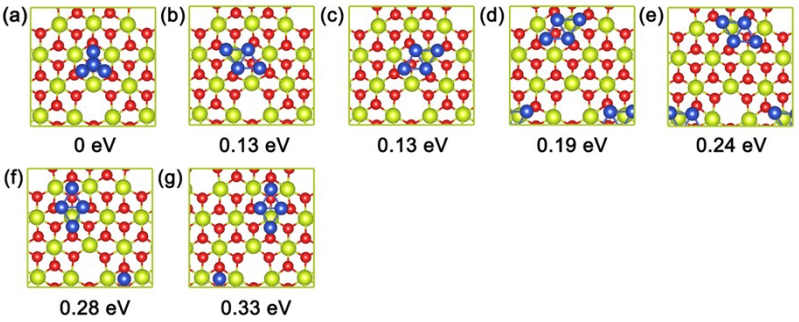

Cu_5/CeO_2-O_v

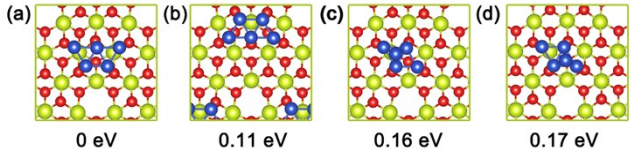

Cu_6/CeO_2-O_v

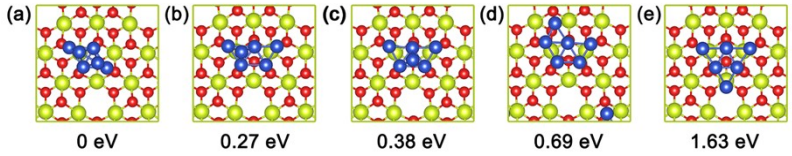

Cu_7/CeO_2-O_v

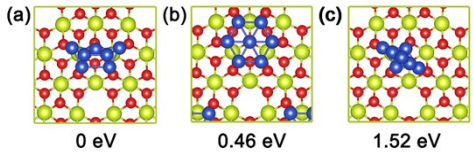

Cu_8/CeO_2-O_v

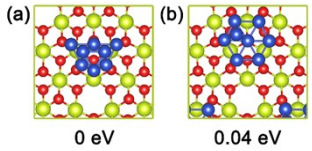

Cu_9/CeO_2-O_v

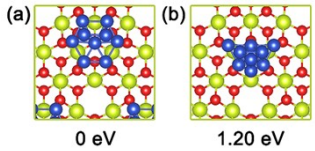

Cu_{10}/CeO_2-O_v

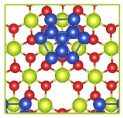

Figure S1. The most stable structure of Cu_n (n = 1-10) clusters anchored at different sites on the surface of CeO_2-O_v, and the values of relative energy are presented at the bottom of the graph. Only a part of the CeO_2-O_v surface is displayed, and Ce, Cu, and O atoms are denoted by cyan, blue and red spheres, respectively.

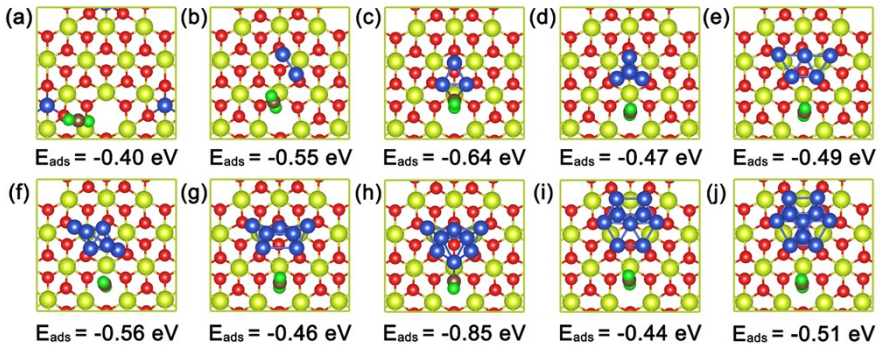

Figure S2. Most stable configuration for the chemisorption of CO_2 molecules at the Cu_n/CeO_2-O_v interface.

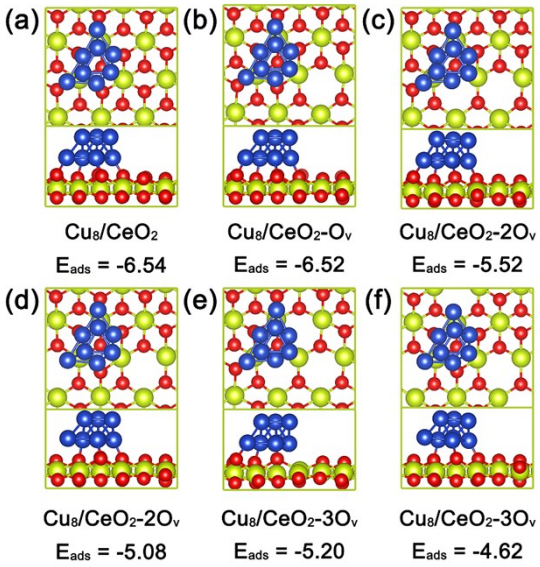

Figure S3. Geometric structure and adsorption energy of Cu_8 on stoichiometric and partially reduced CeO_2 surfaces. n in Cu_8/CeO_2-nO_v is some surface oxygen vacancies in CeO_2 support. Cu_8 adsorption energy (E_{ads}) appears at the bottom, and the unit of adsorption energy is eV.

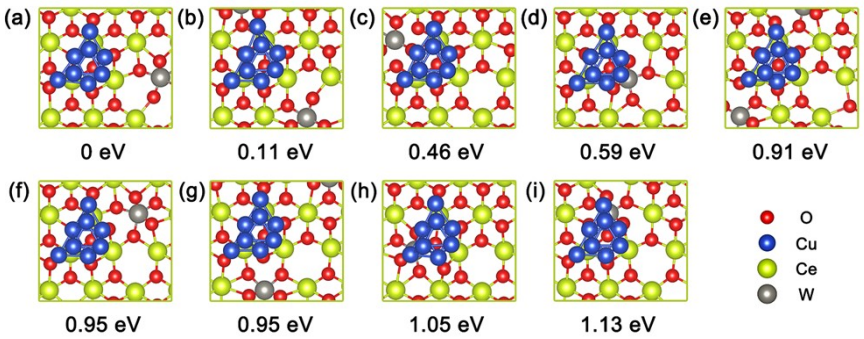

Figure S4. The nine most stable geometries of W-doping on Cu_8/W-CeO_2-O_v (a–i). The values of relative energy are presented at the bottom of the graph.

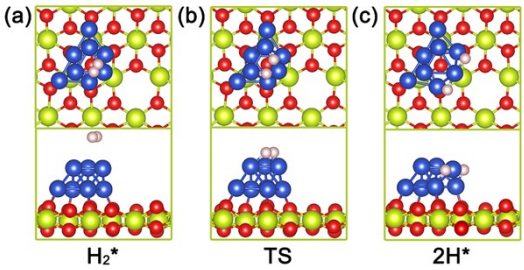

Figure S5. Top and side view of the optimized structures of the initial state (IS), transition state (TS) and final state (FS) involved in the H_2 dissociation path on Cu_8/CeO_2-O_v.

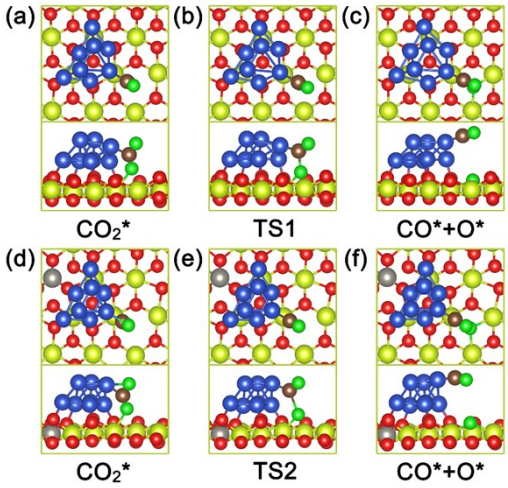

Figure S6. The initial state (IS), transition state (TS) and final state (FS) of the direct dissociation of CO_2* into CO* and O* on Cu_8/CeO_2-O_v and Cu_8/W-CeO_2-O_v, observed from a top view and side view.

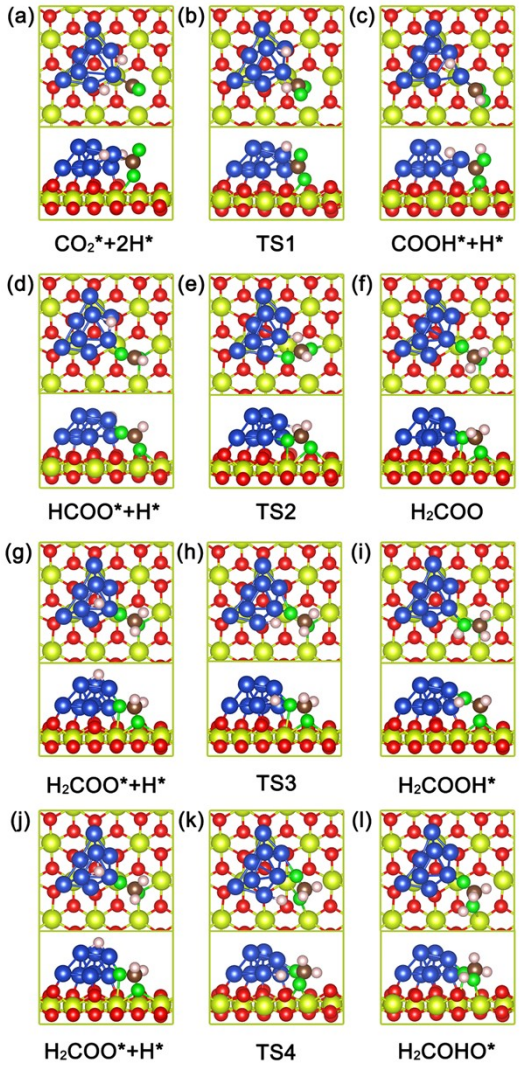

Figure S7. Top and side view of the optimized structures for initial state (IS), transition state (TS) and final state (FS) involved in the higher energy pathway of the formate pathway on Cu_8/CeO_2-O_v.

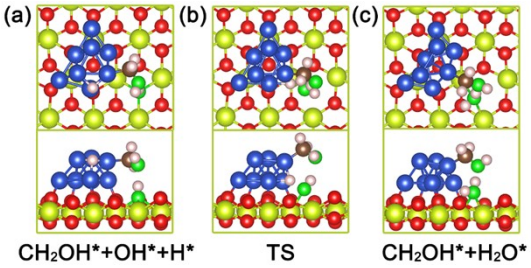

Figure S8. Top and side view of the optimized structures for initial state (IS), transition state (TS) and final state (FS) involved in the generation of H_2O* before the final step (CH_2OH* → CH_3OH*) of the RWGS + CO pathway on Cu_8/CeO_2-O_v.

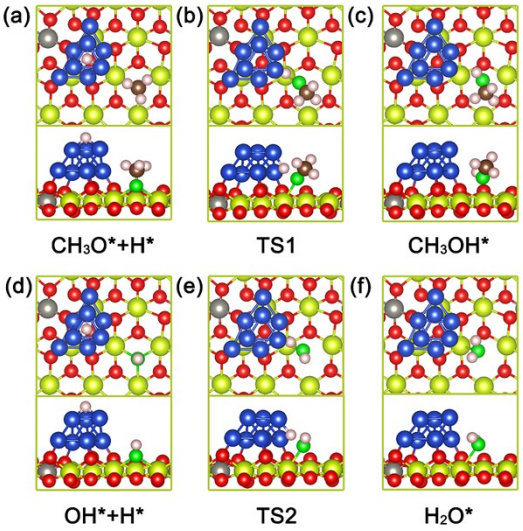

Figure S9. The oxygen vacancy formation step on the Cu_8/W-CeO_2-O_v surface involves the top view and side view of the initial state (IS), transition state (TS) and final state (FS) of CH_3O* hydrogenation to CH_3OH* and OH* hydrogenation to H_2O*.

Table S1. The adsorption energy (E_{ads}, eV) and Bader charge (e) of Cu_n clusters with different sizes on the most stable adsorption configuration of CeO_2-O_v surface.

System	E_{ads}	DDEC charge of Cu atom	DDEC charge of Cu_n clusters
Cu_1/CeO_2-O_v	-3.02	+0.49	+0.49
Cu_2/CeO_2-O_v	-2.59	+0.11 +0.10	+0.21
Cu_3/CeO_2-O_v	-4.90	+0.06 +0.01 +0.01	+0.08
Cu_4/CeO_2-O_v	-5.47	+0.17 +0.15 +0.14 +0.10	+0.56
Cu_5/CeO_2-O_v	-5.79	-0.06 +0.08 +0.07 +0.29 +0.32	+0.70
Cu_6/CeO_2-O_v	-6.09	+0.14 +0.09 +0.17 +0.07 -0.03 -0.01	+0.43
Cu_7/CeO_2-O_v	-6.66	+0.16 +0.19 +0.10 +0.16 -0.02 +0.01	+0.60
Cu_8/CeO_2-O_v	-6.52	+0.11 +0.13 +0.06 +0.11 +0.13 -0.04 -0.04 -0.09	+0.37
Cu_9/CeO_2-O_v	-7.87	+0.12 -0.07 +0.12 -0.02 -0.01 +0.13 +0.08 +0.08 +0.14	+0.57
Cu_{10}/CeO_2-O_v	-8.76	+0.16 +0.04 +0.15 -0.01 -0.01 +0.16 +0.18 +0.16 +0.16 -0.03	+0.96

Table S2. Structural parameters of CO_2 adsorption on Cu_8/CeO_2-O_v and Cu_8/W-CeO_2-O_v models.

Sample	*d* (Cu–C)	*d* (Ce–O_{down})	*d* (C–O_{up})	*d* (C–O_{down})
Cu_8/CeO_2-O_v	2.01	2.60	1.22	1.28
a-Cu_8/W-CeO_2-O_v	2.03	2.59	1.22	1.26
b-Cu_8/W-CeO_2-O_v	--	--	1.17	1.19
c-Cu_8/W-CeO_2-O_v	2.03	2.65	1.22	1.25

Table S3. DFT Calculated reaction energies (E_r/eV) and activation barriers (E_a/eV) for the direct dissociation of CO_2 on Cu_8/CeO_2-O_v and Cu_8/W-CeO_2-O_v Surface.

Sample	reaction	E_r (eV)	E_a (eV)
Cu_8/CeO_2-O_v	CO_2* + * → CO* + O*	+0.50	1.54
Cu_8/W-CeO_2-O_v	CO_2* + * → CO* + O*	+0.59	2.01

Table S4. DFT Calculated reaction energies (E_r/eV) and activation barriers (E_a/eV) for elementary reactions involved in methanol synthesis from CO_2 hydrogenation on Cu_8/CeO_2-O_v Surface.

Step	reaction	E_r (eV)	E_a (eV)
R_1	CO_2* + 2H* → HCOO* + H*	-1.29	0.02
R_2	CO_2* + 2H* → COOH* + H*	-0.70	1.87
R_3	HCOO* + H* → H_2COO* + *	+0.90	1.62
R_4	HCOO* + H* → HCOOH* + *	+1.04	1.08
R_5	HCOOH* + H* → H_2COOH* + *	-0.85	0.19
R_6	H_2COO* + H* → H_2COOH* + *	+0.58	1.78
R_7	H_2COO* + H* → H_2COHO* + *	+1.03	2.93
R_8	H_2COOH* + H* → H_2CO* + H_2O*	+1.12	1.51
R_9	H_2CO* + H_2O* → H_2CO* + H_2O(g) + *	+0.06	--
R_{10}	H_2CO* + H* → H_3CO* + *	-0.70	0.55
R_{11}	H_3CO* + H* → CH_3OH* + *	+0.40	1.18
R_{12}	CH_3OH* → CH_3OH(g) + *	+1.27	--
R_{13}	CO_2* + 2H* → CO* + OH*	-0.69	1.45
R_{14}	CO* + OH* + H* → CHO*+ OH* + *	+0.19	0.96
R_{15}	CO* + OH* + H* → COH*+ OH* + *	+1.73	--
R_{16}	CO* + OH* + H* → CO*+ H_2O* + *	+0.63	1.23
R_{17}	CHO* + OH* + H* → CH_2O* + OH* + *	+0.14	0.84
R_{18}	CHO* + OH* + H* → CH_2O* + H_2O* + *	+0.42	1.58
R_{19}	CH_2O* + OH* + H* → CH_2OH* + OH* + *	-0.45	1.35
R_{20}	CH_2O* + OH* + H* → CH_3O* + OH* + *	+0.14	--
R_{21}	CH_2OH* + OH* + H* → CH_3OH* + OH* + *	-0.25	1.25
R_{22}	CH_2OH* + OH* + H* → CH_2OH* + H_2O * + *	0.25	1.62
R_{23}	OH* + H* → H_2O* + *	+0.48	1.19
R_{24}	CO_3* + 2H* → HCO_3* + H*	-0.09	0.87
R_{25}	HCO_3* + H* → H_2CO_3* + *	+0.92	1.07
R_{26}	H_2CO_3* → H_2CO_3(g) + *	+1.81	--

Table S5. Optimized geometric parameters and adsorption energies of all reaction intermediates on Cu_8/CeO_2-O_v. η-X, X_{bl}, X_a represent the bond length (unit: Å) of the substrate-the nearest adsorbate, the internal bond length (unit: Å) of the adsorbed species, and the internal bond angle (unit: °) of the adsorbed species, respectively. E_{ads} represents the adsorption energy (unit: eV) of the reaction intermediate on the substrate. H^{OH} represents reduction of hydrogen in OH on CeO_2 surface.

species	η-X	d(η-X)	X_{bl}	d(X_{bl})	X_a	angle	E_{ads}
H_Cu	Cu-H	1.624					-0.30
H_CeO_2	O-H	0.975					-1.43
OH	Ce-O	2.593	O-H	0.975			-4.52
H_2O_ Cu	Cu-O	2.021	O-H	1.001	∠HOH	105.9	-0.06
H_2O_CeO_2	Ce-O	2.813	O-H	0.986	∠HOH	100.5	-1.01
CO_2	Cu-C	2.008	C-O_{up}	1.224	∠OCO	132.6	-0.85
	Ce-O	2.599	C-O_{down}	1.277			
HCOO	Cu-O	2.002	C-H	1.111	∠OCO	123.3	-4.54
	Ce-O	2.806	C-O_{up}	1.260	∠HCO_{up}	119.2	
			C-O_{down}	1.283	∠HCO_{down}	117.5	
COOH	Cu-O	1.912	O-H	0.978	∠OCO	112.2	-3.56
	Ce-O	2.762	C-O_{up}	1.360	∠COH	108.0	
			C-O_{down}	1.269			
H_2COO	Cu-O	1.870	C-H	1.113	∠HCH	108.5	-1.56
	Ce-O	2.635	C-O_{up}	1.423	∠OCO	108.7	
		2.629	C-O_{down}	1.410			
HCOOH	Ce-O	2.733	C-H	1.105	∠COH	109.5	-1.39
			O-H	1.016	∠HCO	114.6	
			C-O	1.284	∠OCO	120.6	
H_2COOH	Cu-O	1.974	C-H	1.107	∠HCH	110.3	-3.63
	Ce-O	2.723	O-H	0.985	∠HOC	106.9	
			C-O_{up}	1.517	∠OCO	111.3	
			C-O_{down}	1.356			
H_2CO	Cu-C	2.014	C-H	1.110	∠HCH	112.9	-1.66
	Ce-O	2.699	C-O	1.350	∠HCO	115.1	
CH_2O	Cu-C	2.132	C-H	1.119	∠HCH	115.8	-0.14
	H^{OH}-O		C-O	1.259	∠HCO	120.2	
CH_3O	Ce-O	2.560	C-H	1.111	∠HCH	106.9	-3.50
			C-O	1.417	∠HCO	112.0	
CH_3OH_CeO_2	Ce-O	2.913	C-H	1.101	∠HCH	110.6	-1.27
			C-O	1.452	∠HCO	110.7	
			O-H	0.992	∠HOC	107.0	
CH_3OH_Cu	H^{OH}-O	1.908	C-H	1.104	∠HCH	109.0	-0.09
			C-O	1.430	∠HCO	106.8	
			O-H	0.974	∠HOC	109.1	
CO	Cu-C	1.853	C-O	1.153			-0.97

CHO	Cu-C	1.913	C-H	1.130	∠HCO	116.8	-1.95
	H^{OH}-O	1.927	C-O	1.223			
CH_2OH	Cu-C	1.940	C-H	1.105	∠HCH	109.4	-4.39
	H^{OH}-O	1.842	C-O	1.445	∠HCO	110.3	
			O-H	0.975	∠HOC	108.3	
CO_3	Ce-O	2.601	C-O_a	1.286	∠O_aCO_b	125.7	-13.81
	Cu-O	2.076	C-O_b	1.277	∠O_bCO_c	118.5	
			C-O_c	1.348	∠O_aCO_c	115.3	
HCO_3	Ce-O	2.733	O-H	0.980	∠HO_aC	106.8	-7.99
			C-O_a	1.358	∠O_aCO_b	120.1	
			C-O_b	1.262	∠O_bCO_c	125.0	
			C-O_c	1.290	∠O_aCO_c	114.8	
H_2CO_3	Ce-O	2.740	O-H	1.020	∠HO_aC	111.1	-1.81
			C-O_a	1.324	∠O_aCO_b	119.1	
			C-O_b	1.346	∠O_bCO_c	119.9	
			C-O_c	1.240	∠O_aCO_c	121.0	

Table S6. DFT Calculated reaction energies (E_r/eV) and activation barriers (E_a/eV) for elementary reactions involved in methanol synthesis from CO_2 hydrogenation on Cu_8/W-CeO_2-O_v Surface.

Step	reaction	E_r (eV)	E_a (eV)
R_1	HCOO* + H* → HCOOH* + *	+0.88	1.06
R_2	H_2COOH* + H* → H_2CO* + H_2O*	+0.81	1.01
R_3	CH_3O* + H* → CH_3OH* + *	+0.31	1.22
R_4	CO_2* + H* → CO* + OH*	-0.13	1.99
R_5	OH* + H* → H_2O* + *	+0.44	1.39

Table S7. The density derived electrostatic and chemical (DDEC) charge analysis for Cu_8/CeO_2-O_v, Cu_8/W-CeO_2-O_v, and H_2COOH adsorption on both surfaces.

	C	O_a	O_b	H_a	H_b	H_c	H_2COOH (total)
Cu_8/CeO_2-O_v	+0.30	-0.46	-0.81	0.03	0.05	0.36	-0.53
Cu_8/W-CeO_2-O_v	+0.30	-0.51	-0.84	0.02	0.04	0.33	-0.66

Table S8. The density derived electrostatic and chemical (DDEC) charge analysis for Cu_8/CeO_2-O_v, Cu_8/W-CeO_2-O_v, and CO_2 adsorption on both surfaces.

	C	O_a	O_b	CO_2 (total)
Cu_8/ CeO_2-O_v	+0.46	-0.38	-0.63	-0.55
Cu_8/W-CeO_2-O_v	+0.49	-0.38	-0.57	-0.46

Table S9. The ICOHP value of all adsorbed bonds belonging to the most stable H_2COOH and CO_2 adsorption configuration on Cu_8/CeO_2-O_v and Cu_8/W-CeO_2-O_v.

H_2COOH	Ce-O_{down}	C-O_{up}	Cu-O_{up}	--
Cu_8/CeO_2-O_v	-0.70	-4.03	-0.74	--
Cu_8/W-CeO_2-O_v	-0.84	-4.65	-0.16	--
CO_2	Ce-O_{down}	C-O_{down}	Cu-C	Cu-O_{up}
Cu_8/CeO_2-O_v	-1.34	-6.35	-1.06	-0.04
Cu_8/W-CeO_2-O_v	-1.10	-6.77	-1.00	-0.07

Table S10. TOF values of methanol generated by different catalysts.

Catalyst	T/K	TOF/s^{-1}	Reference
Cu_8/CeO_2-O_v	523	7.1×10^{-6}	this work
Cu_8/W-CeO_2-O_v	523	7.1×10^{-5}	this work
In_2O_3-O_v (110)	473∼573	1×10^{-5}∼1×10^{-1}	[1]
In_2O_3-O_v (111)	473∼573	1×10^{-2}∼1	[1]
Zr1-In_2O_3 (110)	550	1×10^{-4}	[2]
In_2O_3 (110)	550	1×10^{-5}	[2]
Zr3-In_2O_3 (110)	550	1×10^{-8}	[2]
Pt_8/In_2O_3	423∼580	1×10^{-9}∼1×10^{-2}	[3]
Ga_3/Ni_5	500	3.26×10^{-14}	[4]
Cu (211)	523	2.73×10^{-7}	[5]
Cu (211) $_{\text{single-Zn-step}}$	523	3.07×10^{-5}	[5]

[1] Z. Zhou, B. Qin, S. Li, Y. Sun, *Phys*. *Chem*. *Chem*. *Phys*., 2021, **23**, 1888–1895.

[2] K. Li, Z. Wei, Q. Chang, S. Li, *Phys*. *Chem*. *Chem*. *Phys*., 2023, **25**, 14961–14968.

[3] X. Wang, J. Pan, H. Wei, W. Li, J. Zhao, Z. Hu, *J*. *Phys*. *Chem*. *C*, 2022, **126**, 1761–1769.

[4] Q. Tang, Z. Shen, C.K. Russell, M. Fan, *J*. *Phys*. *Chem*. *C*, 2018, **122**, 315–330.

[5] D.Y. Jo, M.W. Lee, H.C. Ham, K.-Y. Lee, *J. Catal*., 2019, **373**, 336–350.